Numerical Assessment of PML Transmission Conditions in a Domain Decomposition Method for the Helmholtz Equation

Niall Bootland, Sahar Borzooei, Victorita Dolean, and Pierre-Henri Tournier

1 Introduction

Finite element discretisations of large-scale time-harmonic wave problems typically lead to ill-conditioned linear systems with a large number of unknowns. A promising class of methods to solve such huge systems in parallel, both in terms of convergence and computing time, is offered by domain decomposition methods (DDMs). These approaches rely on a partition of the computational domain into smaller subdomains, leading to subproblems of smaller sizes which are manageable by direct solvers. A robust domain decomposition (DD) preconditioner for large-scale computations is given in [4]. However, improving the efficiency of such preconditioners continues to be a challenging issue. Recent work has shown that transmission operators based on perfectly matched layers (PMLs) are well-suited for two-dimensional configurations of the Helmholtz problem within non-overlapping DDMs [10]. Further, PMLs have been used successfully as transmission conditions in DDMs applied to geophysical applications modelled by the Helmholtz equation [11].

In this work, we present an efficient PML-based Schwarz-type preconditioner with overlapping subdomains to solve large-scale wave propagation problems. We then assess the performance of this one-level DD algorithm, where the transmission conditions at the boundaries between subdomains are PML conditions in order to

Niall Bootland
STFC Rutherford Appleton Laboratory, Harwell Campus, UK, e-mail: niall.bootland@stfc.ac.uk

Sahar Borzooei
University Côte d'Azur, CNRS, LJAD, France, e-mail: Sahar.Borzooei@univ-cotedazur.fr

Victorita Dolean
University Côte d'Azur, CNRS, LJAD, France, and University of Strathclyde, UK, e-mail: work@victoritadolean.com

Pierre-Henri Tournier
Sorbonne Université, CNRS, Université Paris Cité, Inria, Laboratoire Jacques-Louis Lions (LJLL), F-75005 Paris, France, e-mail: pierre-henri.tournier@sorbonne-universite.fr

provide a better approximation to the transparent boundary operator. Further, we will investigate the convergence properties and compare them with the use of more standard impedance transmission conditions.

2 Mathematical model

As an underlying model we consider the Helmholtz equation in free space, given by

$$-(\Delta + k^2(\mathbf{x}))u(\mathbf{x}) = g(\mathbf{x}), \quad \mathbf{x} \in \Omega \tag{1}$$

for $\Omega = \mathbb{R}^d$ in dimension $d = 2$ or 3, where $k(\mathbf{x}) = \frac{2\pi}{\lambda}$ is the wavenumber, with $\lambda = \frac{c}{f}$ being the wavelength, $c(\mathbf{x})$ the wave speed and f the frequency. Note that the angular frequency is then defined as $\omega = 2\pi f$. To close the problem we prescribe the physically relevant condition at infinity known as the far field Sommerfeld radiation condition

$$\lim_{|\mathbf{x}|\to\infty} |\mathbf{x}|^{\frac{d-1}{2}} \left(\frac{\partial u}{\partial |\mathbf{x}|} - iku \right) = 0. \tag{2}$$

Since we can not compute on the whole free space domain, we consider truncating to an appropriate finite domain. Let us suppose now that $\Omega \subset \mathbb{R}^d$ represents a finite computational domain capturing the physical area of interest. A typical approach, as in [7], is to replace the Sommerfeld condition (2) with the first-order approximation

$$\frac{\partial u}{\partial \mathbf{n}} + iku = 0, \quad \mathbf{x} \in \partial\Omega, \tag{3}$$

known as the impedance (or Robin) boundary condition (Imp BC), with $\mathbf{n}$ being the unit outward normal to the boundary $\partial\Omega$. This enables the appropriate description of wave behaviour in a bounded domain. The finite element discretisation of (1) can then be written as a linear system $A\mathbf{u} = \mathbf{b}$.

2.1 PML formulation

Perfectly matched layers (PMLs) were introduced as a better alternative to absorbing boundary conditions (ABCs) by Berenger [2] to achieve a higher accuracy in domain truncation by eliminating undesired numerical reflections from boundaries, leading to exponential convergence of the numerical solution to the exact solution [1]. PML implementation is done by stretching Cartesian coordinates such that the stretching is defined in a layer surrounding Ω, as in [6], giving a larger computational domain Ω_{PML}. In this regard, we assume the boundaries of the artificially truncated domain Ω are aligned with the coordinate axes.

For simplicity of exposition, we will focus on truncating the problem in the x direction. Let us suppose that the PML extends from the boundary of our domain of interest at $x = a$ to $x = a^*$ and Dirichlet conditions are imposed on $x = a^*$. The stretched coordinate mapping used is given by

$$\frac{\partial}{\partial x_{\text{pml}}} \mapsto \frac{1}{1 - \frac{i}{\omega}\sigma(x)} \frac{\partial}{\partial x}, \quad \text{where} \quad \begin{cases} \sigma(x) = 0 & \text{if } x < a, \\ \sigma(x) > 0 & \text{if } a < x < a^*. \end{cases} \tag{4}$$

In the PML region, where $\sigma(x) > 0$, oscillating solutions turn into exponentially decaying ones. In the original domain Ω, $\sigma(x) = 0$ so that the underlying equation is unchanged. In this work we will study three different stretching functions [3, 8], namely

$$\sigma_{-1}(x) = \frac{1}{a^* - x}, \quad \sigma_{-2}(x) = \frac{2}{(a^* - x)^2}, \quad \text{and} \quad \sigma_2(x) = \alpha(a^* - x)^2. \tag{5}$$

In $\sigma_2(x)$, α is experimentally chosen to take the value 30 in our simulations. To incorporate a PML into other coordinate directions, we simply apply equivalent one-dimensional transformations to obtain $\frac{\partial}{\partial y_{\text{pml}}}$ and $\frac{\partial}{\partial z_{\text{pml}}}$. At the corners of the extended computational domain Ω_{PML} we will have PML regions that stretch along two or three directions simultaneously; this will not generate any problems. Implementing this mapping in, for instance, a three-dimensional domain requires a slight change to the Helmholtz equation (1) over Ω_{PML}, resulting in the Laplace operator Δ being replaced by following operator which stretches in the PMLs

$$\Delta_{\text{pml}} = \frac{\partial^2}{\partial {x_{\text{pml}}}^2} + \frac{\partial^2}{\partial {y_{\text{pml}}}^2} + \frac{\partial^2}{\partial {z_{\text{pml}}}^2}. \tag{6}$$

2.1.1 Accuracy assessment for PMLs

In this section we will solve the Helmholtz equation when PMLs are applied as global boundary conditions for a 2D domain of length 10λ in each direction. We will compute the L^2 relative error with respect to the analytical exact solution and compare it with the situation where impedance boundary conditions are used instead. We consider a scattering problem of a plane wave by a circular obstacle, with a Dirichlet boundary condition on the boundary of the obstacle, shown in Figure 1. First, in Table 1, we compare different stretching functions σ with the utilization of higher order P3 Lagrange finite elements and discretization of $n_\lambda = 20$ points per wavelength. We find that the best accuracy is obtained with σ_{-1} and so we continue our tests with this function here. Within our tests we vary the number of points per wavelength n_λ and the PML length in order to investigate their relative effect on the resulting error. Results are detailed in Table 2. We see that, except for $n_\lambda = 5$, PMLs provide higher accuracy compared to impedance boundary conditions, even when the length of the PMLs incorporate only 0.1λ. Moreover, for a fixed PML length,

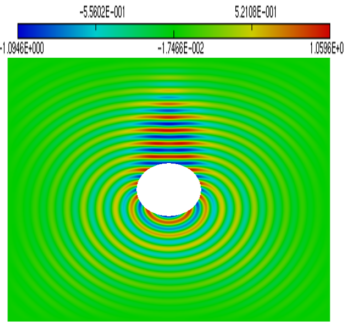

Fig. 1 Plane wave excitation solution when using PMLs as global boundary conditions in 2D.

Table 1 L^2 relative error for different stretching functions σ with PML length $L_{\text{pml}} = \lambda$. The radius of the circular obstacle is $R = \lambda$.

Stretching functions		
σ_{-1}	σ_{-2}	σ_2
0.00112	0.001517	0.075495

Table 2 L^2 relative error for different PML lengths with σ_{-1} or impedance boundary conditions (Imp BCs), $R = \lambda$.

	PML length										
n_λ	0.1λ	0.2λ	0.3λ	0.5λ	λ	2λ	3λ	4λ	5λ	10λ	Imp BCs
5	0.10408	0.02441	0.02684	0.02120	0.01685	0.01251	0.00927	0.00741	0.00605	0.00265	0.05118
10	0.01354	0.01011	0.00665	0.00534	0.00425	0.00311	0.00235	0.00184	0.00150	0.00067	0.04642
20	0.00893	0.00467	0.00268	0.00159	0.00112	0.00078	0.00059	0.00046	0.00038	0.00017	0.04620
30	0.00797	0.00320	0.00175	0.00083	0.00050	0.00035	0.00026	0.00021	0.00017	0.00007	0.04620
40	0.00617	0.00246	0.00121	0.00056	0.00029	0.00020	0.00015	0.00012	0.00009	0.00006	0.046212
50	0.00578	0.00192	0.00096	0.00041	0.00020	0.00013	0.00010	0.00008	0.00006	0.00003	0.046216

and again even for 0.1λ, the error still decreases when increasing n_λ, whereas for impedance boundary conditions the error is dominated by the domain truncation even for $n_\lambda = 5$. Of course, the error also decreases significantly with increasing PML length, all the way down to 3×10^{-5} for $n_\lambda = 50$ and 10λ.

2.2 Domain decomposition preconditioner

A preconditioner M^{-1} is a linear operator whose use aims to reduce ill-conditioning and allow faster convergence of an iterative solver. Usually (but not always) this approximates A^{-1} and has a matrix–vector product that is much cheaper to compute than solving the original linear system. To this end, we employ right preconditioning within GMRES to solve our discretised linear system, namely by solving

$$AM^{-1}\mathbf{y} = \mathbf{f}, \quad \text{where} \quad \mathbf{u} = M^{-1}\mathbf{y}. \tag{7}$$

Right preconditioning benefits from minimising a residual that is independent of the preconditioner, unlike left-preconditioned GMRES. Overlapping Schwarz methods come with the advantages of better convergence and easier implementation compared to substructuring methods. Furthermore, contrary to non-overlapping methods, corners do not need specific treatment. Overlapping methods are also a natural choice to consider when using PML transmission conditions, as the added PML can be naturally included in the overlap region. In this work we use the optimised restricted additive Schwarz (ORAS) domain decomposition preconditioner, given by

$$M_{\text{ORAS}}^{-1} = \sum_{s=1}^{N_{\text{sub}}} R_s^T D_s A_s^{-1} R_s, \tag{8}$$

where N_{sub} is the number of overlapping subdomains Ω_s into which the domain Ω is decomposed. To define the matrices present in (8), let $\mathcal{N}$ be an ordered set of the unknowns of the whole domain and let $\mathcal{N} = \bigcup_{s=1}^{N_{\text{sub}}} \mathcal{N}_s$ be its decomposition into the non-disjoint ordered subsets corresponding to the different overlapping subdomains Ω_s. Further, define $N = |\mathcal{N}|$ and $N_s = |\mathcal{N}_s|$. The $N_s \times N_s$ matrices A_s stem from the discretisation of local boundary value problems on Ω_s with transmission conditions chosen as either Robin or PML conditions to be implemented at the subdomain interfaces. The $N_s \times N$ matrix R_s is the Boolean restriction matrix from Ω to subdomain Ω_s while R_s^T is then the extension matrix from subdomain Ω_s to Ω. The $N_s \times N_s$ diagonal matrices D_s provide a discrete partition of unity, i.e., are such that $\sum_{s=1}^{N_{\text{sub}}} R_s^T D_s R_s = I$. See, e.g., [5, 9] for further details on such methods. PMLs are introduced as transmission conditions on the interface boundaries of the local subdomains in [10]. In this approach, the PML region is included strictly inside the overlap, the PML region being the outermost layers within each overlapping domain. This ensures that there is enough overlap for the approach to be efficient and sufficient length of the PML for a good approximation of the interface transmission condition.

3 Numerical results

3.1 PML as transmission conditions for a 2D domain

As a simple model, we consider excitation by a Gaussian point source, $S(x, y) = e^{-30k((x-5)^2+(y-5)^2)}$, in the center of a 2D domain of size $[0, 10] \times [0, 10]$, as shown in Figure 2 (left). The convergence rate is studied when either PML or impedance conditions are imposed as global boundary conditions (BCs) or interface conditions (ICs). This leads to four different configurations in total[1]. To discretise we employ P3 finite elements on regular grids with $n_\lambda = 15$.

[1] In 2D we present results only with PMLs for the global BCs; a comparison with impedance BCs will be given later for the full 3D problem in Table 5.

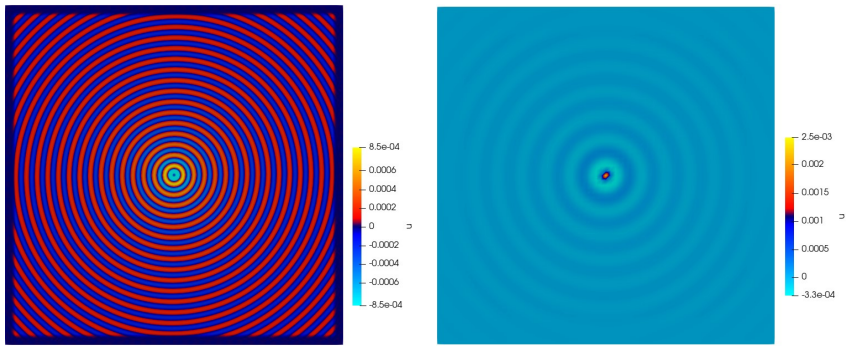

Fig. 2 The solution of the 2D, with $f = 3Hz$ (left), and 3D, with $f = 1Hz$ (right), point source excitation problem with PML boundary conditions.

In our tests, we set the wave speed to $c = 1$ and we vary the frequency f from 3Hz to 10Hz, which leads to a number of wavelengths in the domain ranging from 30 to 100. That also results in different values of #DoFs, which represents the number of degrees of freedom in the discrete problem. We decompose the global domain into either $N = 8 \times 8 = 64$ or $N = 10 \times 10 = 100$ square subdomains and use interface PML regions of length L_{pmli}.

In Table 3, simulations results are given using the σ_{-1} stretching function[2], where the interface PML length is $L_{\text{pmli}} = 1h$ and $h = \frac{\lambda}{n_\lambda}$ is the mesh size. The PML length on the global boundary is chosen to be $L_{\text{pml}} = 2\lambda$ and the number of overlapping layers of elements between subdomains is varied from 2 to 8 layers. We first observe that when interface PMLs are used we always require fewer iterations compared to using impedance ICs. Secondly, with the impedance condition the iteration counts increase with frequency f, but this is not the case when using interface PMLs where iteration counts remain insensitive to f. Finally, we note that an overlap of 4 layers is sufficient here for the PMLs with little benefit seen as we increase the overlap further while for the impedance condition a larger overlap is needed to continually reduce the iteration counts.

In Table 4, the simulations with $f = 3$ Hz are repeated but now with $L_{\text{pmli}} = 5h$. Note that for the appropriate transmission of data between subdomains, we should consider the length of the overlap to be larger than the length of the PML region. This can be seen in Table 4 where an overlap of more than 5 layers is required for good convergence. Comparing the number of iterations, when the overlap is sufficient, with those in Table 3, we can see a small improvement in the convergence when using a larger interface PML region. Note that the one-level preconditioner is by nature not robust, in the sense that the number of iterations usually depends on the number of subdomains. That is to say, the number of iterations does not depend only on the quality of the approximation of the absorbing interface conditions, which as we can see from Table 2 is already good when using PMLs of small length.

[2] A comparison with other choices of stretching function σ will be given later in Table 7.

Table 3 Iteration counts for varying frequency f and choices of ICs, discretised using P3 elements with $n_\lambda = 15$. Within the PMLs we use σ_{-1}, $L_{\text{pmli}} = 1h$ and $L_{\text{pml}} = \lambda$.

				Overlap							
				$N = 64$				$N = 100$			
BCs	ICs	f (Hz)	#DoFs	2	4	6	8	2	4	6	8
PML	Imp	3	2,076,481	52	48	44	41	65	58	53	51
PML	PML			39	33	33	32	49	42	40	42
PML	Imp	5	5,480,281	63	59	56	54	70	65	60	57
PML	PML			41	35	33	34	49	42	41	42
PML	Imp	10	21,077,281	69	67	63	61	77	71	67	68
PML	PML			40	34	33	34	48	41	41	41

Table 4 Iteration counts for $f = 3\,Hz$ and varying choices of ICs, discretised using P3 elements with $n_\lambda = 15$. Within the PMLs we use σ_{-1}, $L_{\text{pmli}} = 5h$ and $L_{\text{pml}} = \lambda$.

				Overlap							
				$N = 64$				$N = 100$			
BCs	ICs	f (Hz)	#DoFs	2	4	6	8	2	4	6	8
PML	Imp	3	2,076,481	52	48	44	41	65	58	53	51
PML	PML			110	64	31	31	140	80	39	39

3.2 PML as transmission conditions for a 3D domain

In this section, we consider a similar Gaussian point source excitation in the center of the 3D domain, $S(x, y, z) = e^{-30k((x-5)^2+(y-5)^2+(z-5)^2)}$; see Figure 2 (right). For this problem we discretise with P2 finite elements and use $n_\lambda = 5$ and $L_{\text{pml}} = 2\lambda$. When recording iteration counts in this section, the use of – means the simulation failed due to memory limitations while • indicates a lack of convergence in 2000 iterations. In Table 5 we use σ_{-1} and compare all four combinations of BCs and ICs when $L_{\text{pmli}} = 1h$ and $f = 1\,\text{Hz}$, this results in #DoFs = 2,803,221. We observe that using PML rather than impedance conditions reduces iteration counts both when used as BCs or ICs, in particular, when swapping from impedance for both BCs and ICs to PMLs we see at least a $2/3$ reduction in iterations. Furthermore, using PML BCs again provides a somewhat more accurate solution when comparing L^2 relative error with respect to the analytical exact solution. Here, we consider $N = 6 \times 6 \times 5 = 180$ and $N = 7 \times 7 \times 6 = 294$ subdomains.

In Table 6, simulations for the full PML case are repeated for different lengths of L_{pmli}. Again we see the overlap should be larger than the interface PML length and, when so, iteration counts slowly decrease as L_{pmli} increases.

Finally, we compare different stretching functions σ for the case of $L_{\text{pmli}} = 4h$. The results in Table 7 show that the best convergence is provided when we choose σ_{-1}. While the iteration counts when using σ_{-2} have only a small increase, it is always more effective to use σ_{-1}. The convergence observed for σ_2 is much poorer, demon-

Table 5 Iteration counts and L^2 error for $f = 1$ Hz and varying choices of BCs and ICs, discretised using P2 elements with $n_\lambda = 5$. Within the PMLs we use σ_{-1}, $L_{\text{pmli}} = 1h$ and $L_{\text{pml}} = 2\lambda$.

		Overlap								
		$N = 180$				$N = 294$				
BCs	ICs	2	4	6	8	2	4	6	8	L^2 relative error
Imp	Imp	40	31	27	–	45	35	32	34	0.211853
Imp	PML	36	29	26	–	42	35	29	31	
PML	Imp	30	22	20	–	33	25	23	21	0.0709828
PML	PML	24	20	18	–	27	23	20	19	

Table 6 Iteration counts for $f = 1$ Hz with PML BCs and ICs varying the PML interface length L_{pmli}, discretised using P2 elements with $n_\lambda = 5$. Within the PMLs we use σ_{-1} and $L_{\text{pml}} = 2\lambda$.

			Overlap							
			$N = 180$				$N = 294$			
BCs	ICs	L_{pmli}	2	4	6	8	2	4	6	8
PML	PML	$1h$	24	20	18	–	27	23	20	19
PML	PML	$2h$	30	19	17	–	34	22	19	18
PML	PML	$4h$	37	21	15	–	42	24	17	15
PML	PML	$6h$	38	21	18	–	43	24	21	15

Table 7 Iteration counts for $f = 1$ Hz and varying choice of ICs and PML stretching function σ, discretised using P2 elements with $n_\lambda = 5$. Within the PMLs we use $L_{\text{pmli}} = 4h$ and $L_{\text{pml}} = 2\lambda$.

			Overlap							
		Stretching	$N = 180$				$N = 294$			
BCs	ICs	function	2	4	6	8	2	4	6	8
PML	Imp	σ_{-1}	30	22	20	–	33	25	23	21
PML	PML		37	21	15	–	42	24	17	15
PML	Imp	σ_{-2}	33	28	24	–	38	30	27	26
PML	PML		•	33	19	–	•	38	23	19
PML	Imp	σ_2	•	•	973	–	•	•	1984	1201
PML	PML		•	•	•	–	•	•	•	•

strating the importance of choosing a suitable stretching function in order to be advantageous in the domain decomposition preconditioner. In our tests σ_{-1} provided the best choice and justifies its use in our previous simulations.

4 Conclusion

In this work, we have introduced the use of PMLs as interface conditions within an overlapping domain decomposition solver for Helmholtz equations. With the choice of PMLs as interface conditions, better convergence is achieved compared to using impedance conditions. Results on 2D and 3D model problems show the utility of the approach with a suitable choice of stretching function.

References

1. Bao, G. and Wu, H. Convergence analysis of the perfectly matched layer problems for time-harmonic maxwell's equations. *SIAM journal on numerical analysis* **43**(5), 2121–2143 (2005).
2. Berenger, J.-P. A perfectly matched layer for the absorption of electromagnetic waves. *Journal of computational physics* **114**(2), 185–200 (1994).
3. Bermudez, A., Hervella-Nieto, L., Prieto, A., and Rodríguez, R. Perfectly matched layers for time-harmonic second order elliptic problems. *Archives of Computational Methods in Engineering* **17**, 77–107 (2010).
4. Bonazzoli, M., Dolean, V., Graham, I., Spence, E., and Tournier, P.-H. Domain decomposition preconditioning for the high-frequency time-harmonic maxwell equations with absorption. *Mathematics of Computation* **88**(320), 2559–2604 (2019).
5. Bonazzoli, M., Dolean, V., Hecht, F., and Rapetti, F. Overlapping schwarz preconditioning for high order edge finite elements: Application to the time-harmonic maxwell's equations (2016).
6. Borzooei, S., Dolean, V., Migliaccio, C., Tournier, P.-H., and Pichot, C. A fast and precise parallel numerical model using pml for maxwell's equations. In: *2022 IEEE International Symposium on Antennas and Propagation and USNC-URSI Radio Science Meeting (AP-S/URSI)*, 153–154. IEEE (2022).
7. Borzooei, S., Dolean, V., Tournier, P.-H., and Migliaccio, C. Solution of time-harmonic maxwell's equations by a domain decomposition method based on pml transmission conditions. *arXiv preprint arXiv:2211.04912* (2022).
8. Marburg, S. and Nolte, B. *Computational acoustics of noise propagation in fluids: finite and boundary element methods*, vol. 578. Springer (2008).
9. Nataf, F. Interface connections in domain decomposition methods. *Modern methods in scientific computing and applications* 323–364 (2002).
10. Royer, A., Geuzaine, C., Béchet, E., and Modave, A. A non-overlapping domain decomposition method with perfectly matched layer transmission conditions for the helmholtz equation. *Computer Methods in Applied Mechanics and Engineering* **395**, 115006 (2022).
11. Tournier, P.-H., Jolivet, P., Dolean, V., Aghamiry, H. S., Operto, S., and Riffo, S. 3d finite-difference and finite-element frequency-domain wave simulation with multilevel optimized additive schwarz domain-decomposition preconditioner: A tool for full-waveform inversion of sparse node data sets. *Geophysics* **87**(5), T381–T402 (2022).